

Supporting Information for

Photolysis of BODIPY Dye Activated by Pillar[5]arene

Haifan Zhang,^a Long Wang,^a Puyang Dong,^a Shuqiang Mao,^a Pu Mao^{*a} and Guoxing Liu^{*ab}

^aCollege of Chemistry and Chemical Engineering, Henan University of Technology, Zhengzhou 450001, P. R. China

^bCollege of Science, Henan Agricultural University, Zhengzhou, Henan 450002, China

*E-mail: gxliu@henau.edu.cn

maopu@haut.edu.cn

Table of Contents

1. Materials and measurements.
2. The determination of photochemical quantum yield.
3. Synthesis, NMR spectrum and HR-MS.
4. The variation of ^1H NMR spectra of **G-BODIPY** with continuous addition of **P5**.
5. The UV/vis absorption spectra of **G-BODIPY** with continual addition of **P5**.
6. The fluorescence spectra of **G-BODIPY** with continual addition of **P5**.
7. The variation of ^1H NMR spectra of **G-BODIPY** \subset **P5**₂ upon continuous irradiation of 311 nm.
8. HR-MS (ESI) spectra of **P5** and **G-BODIPY** \subset **P5**₂ before and after irradiation at 311 nm light.
9. The variation of ^1H NMR spectra of **G-BODIPY** upon continuous irradiation of 311 nm.
10. The variation of UV-vis absorption spectra of **P5** and **PDME** upon continuous irradiation of 311 nm light.
11. The UV/vis absorption spectra of **P5** and **PDME**.
12. The variation of UV-vis absorption and fluorescence spectra of **G-BODIPY** and **G-BODIPY** \subset **P5**₂ (b) upon continuous irradiation of 500 nm light.
13. The fluorescence spectra of **P5** and **G-BODIPY** \subset **P5**₂.
14. Spectral overlap of the absorption of **G-BODIPY** and the fluorescence emission of **P5**.
15. The variation of UV-vis absorption spectra of **P5** and **G-BODIPY** \subset **P5**₂ in an oxygenated environment and a deoxidized environment upon continuous irradiation of 311 nm light.
16. The variation of UV-vis absorption spectra of **G-BODIPY** \subset **P5**₂ in absence of TEMPO and in presence of TEMPO with irradiation time of 311 nm light.
17. The variation of UV-vis absorption and fluorescence spectra of **4** and **4+P5** upon continuous irradiation of 311 nm light.
18. Association constant determination for the complexation between **G** and **H**.

Materials and measurements

All manipulations were carried out under an argon atmosphere by using standard Schlenk techniques, unless otherwise stated. THF was distilled under argon atmosphere from sodium-benzophenone. All other starting materials were obtained commercially as analytical-grade and used without further purification. ^1H NMR and ^{13}C NMR spectra were recorded on a Bruker DPX 400 spectrometer with TMS as the internal standard at 25 °C. Mass spectra were measured in the ESI mode. The UV-vis absorption spectra were measured in a quartz cell (light path, 10 mm or 1 mm) on UNICO UV-4802. Steady-state fluorescence spectra were recorded in a conventional quartz cell (light path, 10 mm) on HITACHI F-7000 FL. The Philips UVB 311nm (9 W, Single wavelength) was employed to perform the photochemistry experiment at room temperature. Irradiation experiments ($\lambda = 500$ nm) was carried out using a CEL-HXF300 20V 300W xenon lamp (Beijing China Education Au-light Co. Ltd., China) with a band-pass optical filter (CEL-QD500) for 500 nm light (Beijing China Education Au-light Co. Ltd., China) at room temperature.

The determination of photochemical quantum yield (Φ) of G-BODIPY-C₅P₂

The photon flux of the Philips UVB 311nm (9 W, Single wavelength) was estimated by measuring the production of ferrous ions from potassium ferrioxalate. 3 mL of 0.006 M solution of potassium ferrioxalate in 0.005 M H_2SO_4 was irradiated for 30 s. At the end of the irradiation, 0.5 mL of buffered phenanthroline solution was added in the cells and the absorbance at 510 nm measured after one hour. According to the experiment, the rate (r) of Fe^{2+} ion formation calculated to be $9.08 \times 10^{-6} \text{ M s}^{-1}$. The moles of photons absorbed per time unit ($Nh/t = \text{moles of Fe}^{2+}/t$) in a 3 mL solution can be calculated using the reported quantum yield of ferrioxalate ($\Phi_{311\text{nm}} = 1.24$).

G-BODIPYC₅P₂ in CHCl₃ (2×10^{-5} M) in 1 cm quartz cuvette was irradiated by a Philips UVB 311nm (9 W, Single wavelength) at 20°C. The absorbance decrease at $\lambda = 503$ nm was monitored over time by UV-vis spectroscopy and the molar absorptivities at this wavelength ($\epsilon = 10633 \text{ M}^{-1} \text{ cm}^{-1}$) were used to calculate the concentration of photodecomposition efficiency. The slopes for the plots of the concentration decrease versus time, at low conversion, represent the rate of photodecomposition (r). These were obtained by linear fitting to the equation $y = ax + b$ using Origin software. The photochemical quantum yield was obtained by comparison of the rate for reduction of **G-BODIPY** ($r = 2.53 \times 10^{-6} \text{ M s}^{-1}$) with the rate of Fe²⁺ formation from potassium ferrioxalate giving $\Phi = 0.34$.

Synthesis of G-BODIPY

Compound **4** (172 mg, 0.40 mmol) and compound **5** (99 mg, 0.80 mmol) were dissolved in a mixture of THF (16 mL) and water (4 mL). Then CuSO₄·5H₂O (40 mg, 0.16 mmol) and sodium ascorbate (64 mg, 0.32 mmol) were added and the mixture was stirred at room temperature for 24 h. Then the mixture was diluted with water (10 mL) and extracted by DCM (3×20 mL). The combined organic extracts were dried over anhydrous Na₂SO₄ and concentrated under reduced pressure. The crude product was purified by column chromatography (silica gel, DCM) to give *G-BODIPY* as an orange-red solid. Yield: 114 mg, 42%. ¹H NMR (400 MHz, CDCl₃, 298 K) δ ppm = 7.86 (s, 1H), 7.76 (s, 1H), 7.16 (d, $J = 8.4$ Hz, 1H), 6.93 (d, $J = 1.6$ Hz, 1H), 6.86 (dd, $J = 8.2, 1.6$ Hz, 1H), 5.97 (s, 2H), 5.26 (d, $J = 39.2$ Hz, 4H), 4.46-4.40 (m, 4H), 2.54 (s, 6H), 2.44-2.38 (m, 4H), 2.13-2.04 (m, 4H), 1.73-1.64 (m, 4H), 1.39 (s, 6H). ¹³C NMR (100

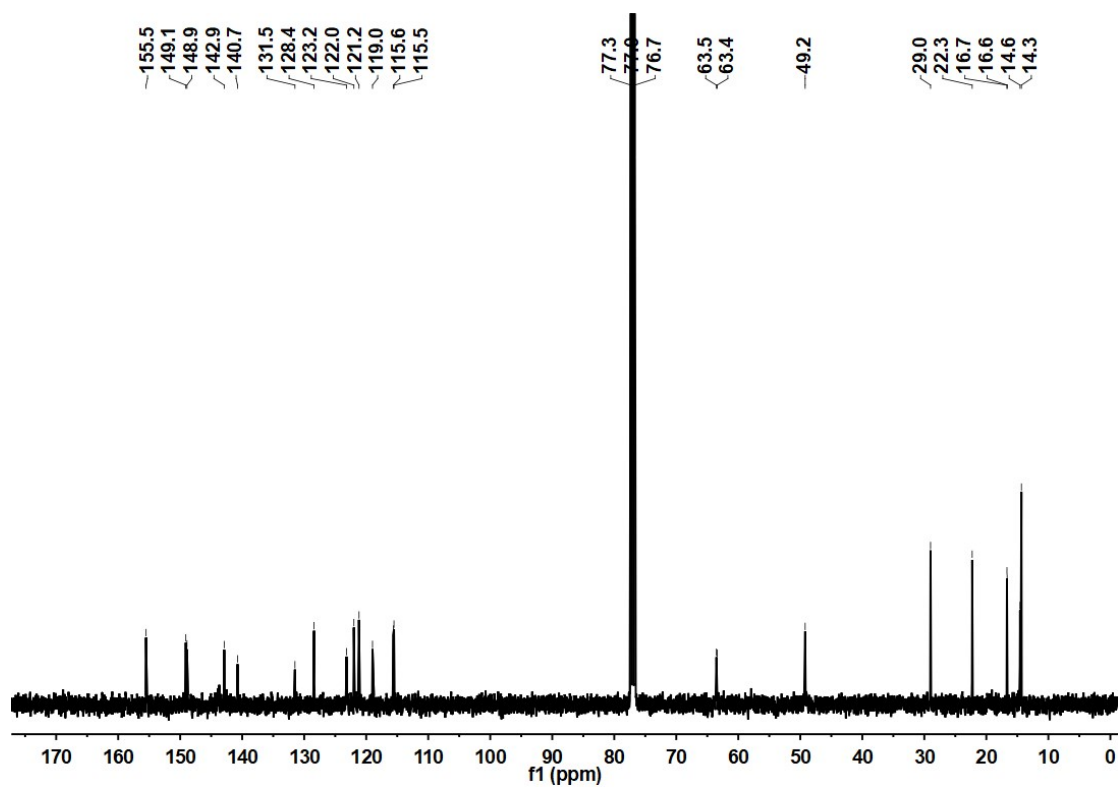


Figure S2. ^{13}C NMR spectrum (400 MHz, 298 K, CDCl_3) of **G-BODIPY**.

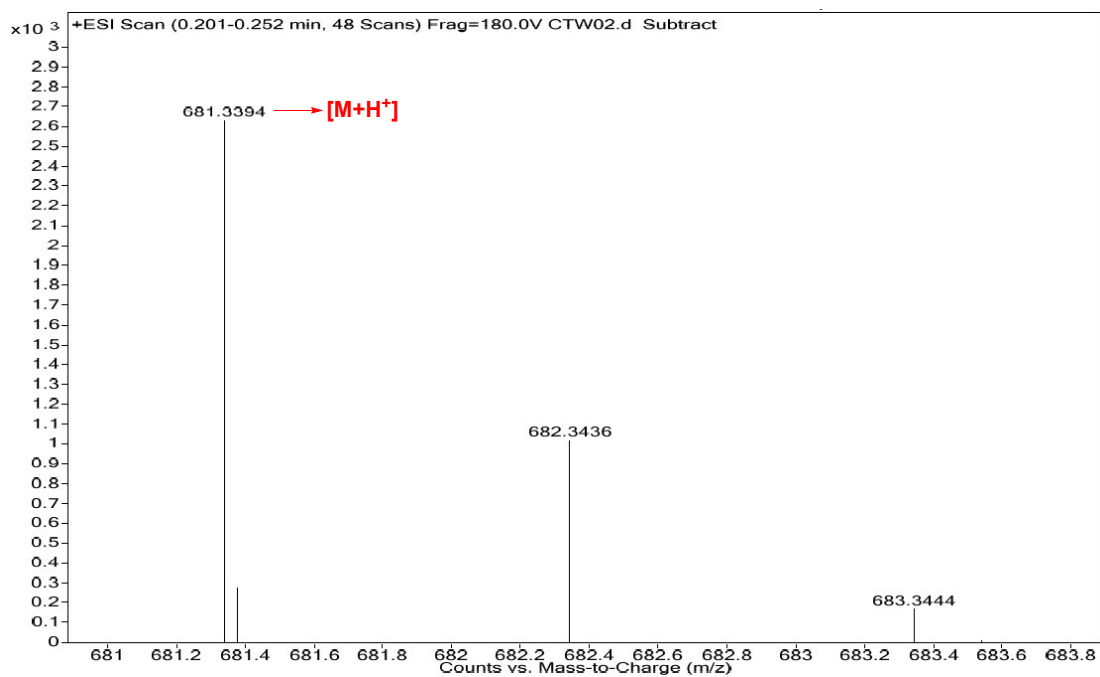


Figure S3. HR-MS(ESI) spectrum of **G-BODIPY**.

Synthesis of P5

The synthesis of **P5** was prepared by literature method.¹

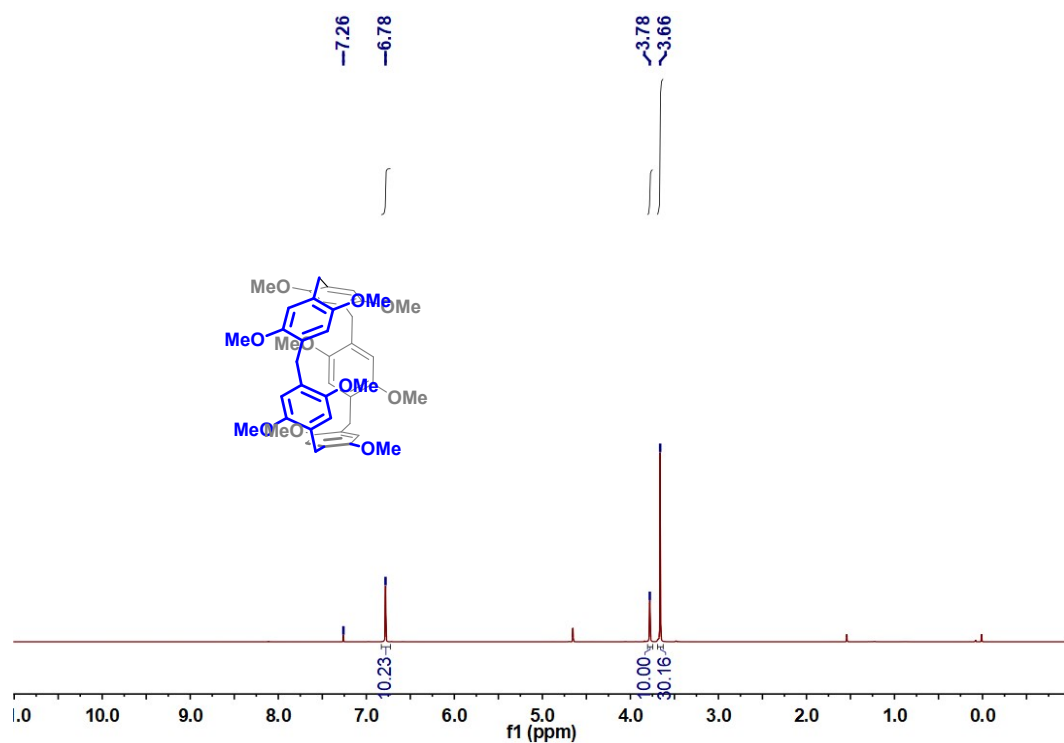


Figure S4. ¹H NMR spectrum (400 MHz, 298 K, CDCl₃) of P5.

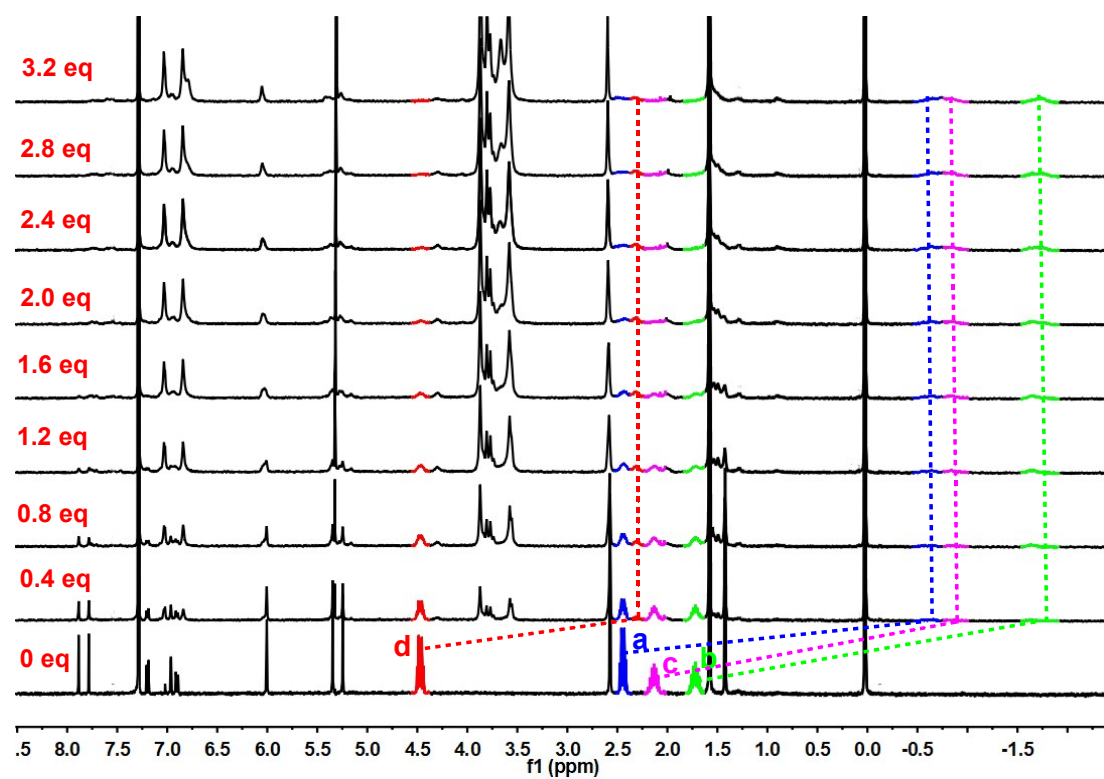


Figure S5. The variation of ¹H NMR (400 MHz, 298 K, CDCl₃) spectra of G-BODIPY with continuous addition of P5. ([G-BODIPY] = 3.0 × 10⁻³ M)

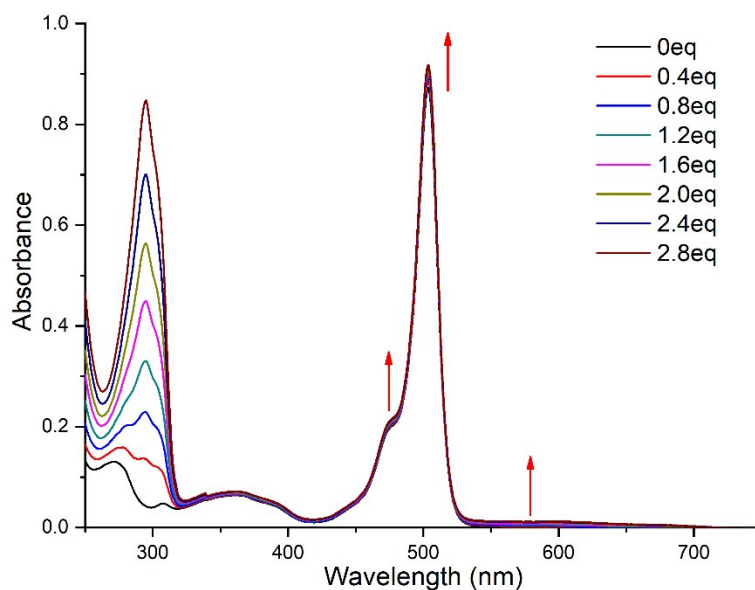


Figure S6. The UV/vis absorption spectra of **G-BODIPY** with sequential addition of 0 – 2.8 eq **P5**; $[\text{G-BODIPY}] = 1 \times 10^{-5} \text{ mol/L}$.

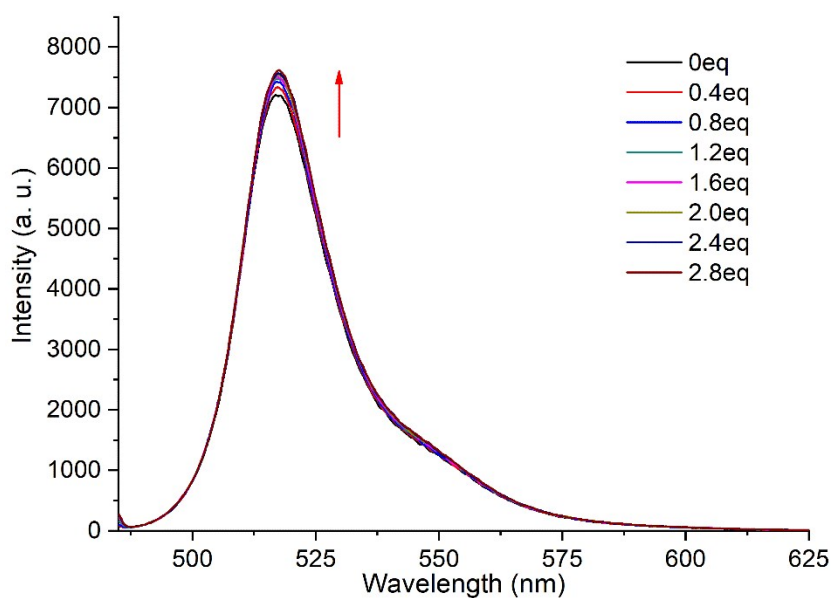


Figure S7. The fluorescence spectra of **G-BODIPY** with addition of 0 – 2.8 eq **P5**; $[\text{G-BODIPY}] = 1 \times 10^{-5} \text{ mol/L}$; Excitation at 480 nm; Slit = 1, 2.5.

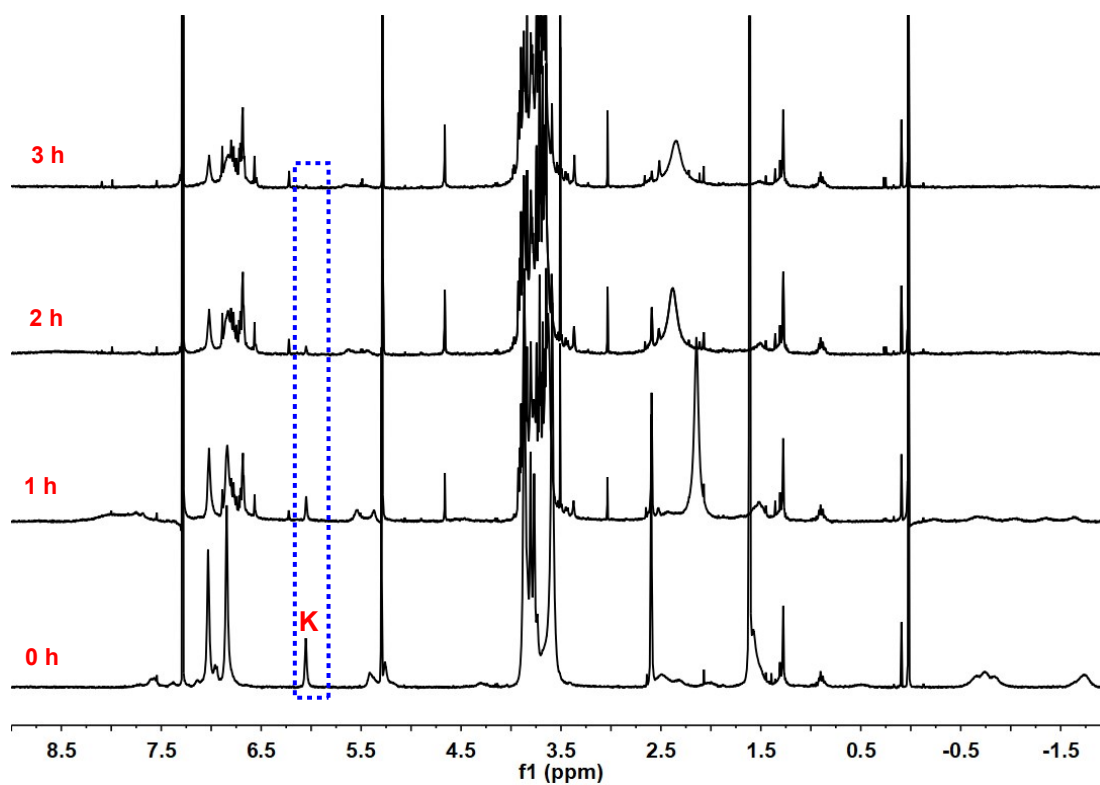


Figure S8. The variation of ^1H NMR (400 MHz, 298 K, CDCl_3) spectra of **G-BODIPY-P5** upon continuous irradiation of 311 nm for 1 h, 2 h and 3 h.

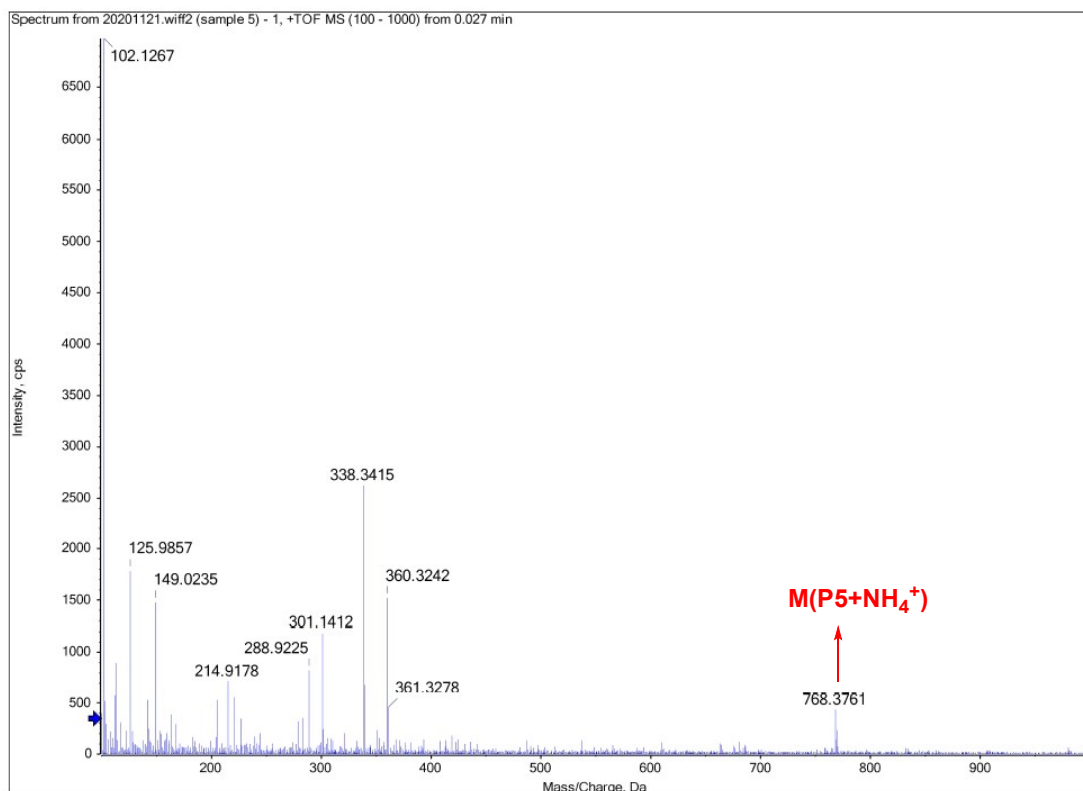


Figure S9. HR-MS (ESI) spectrum of **P5**.

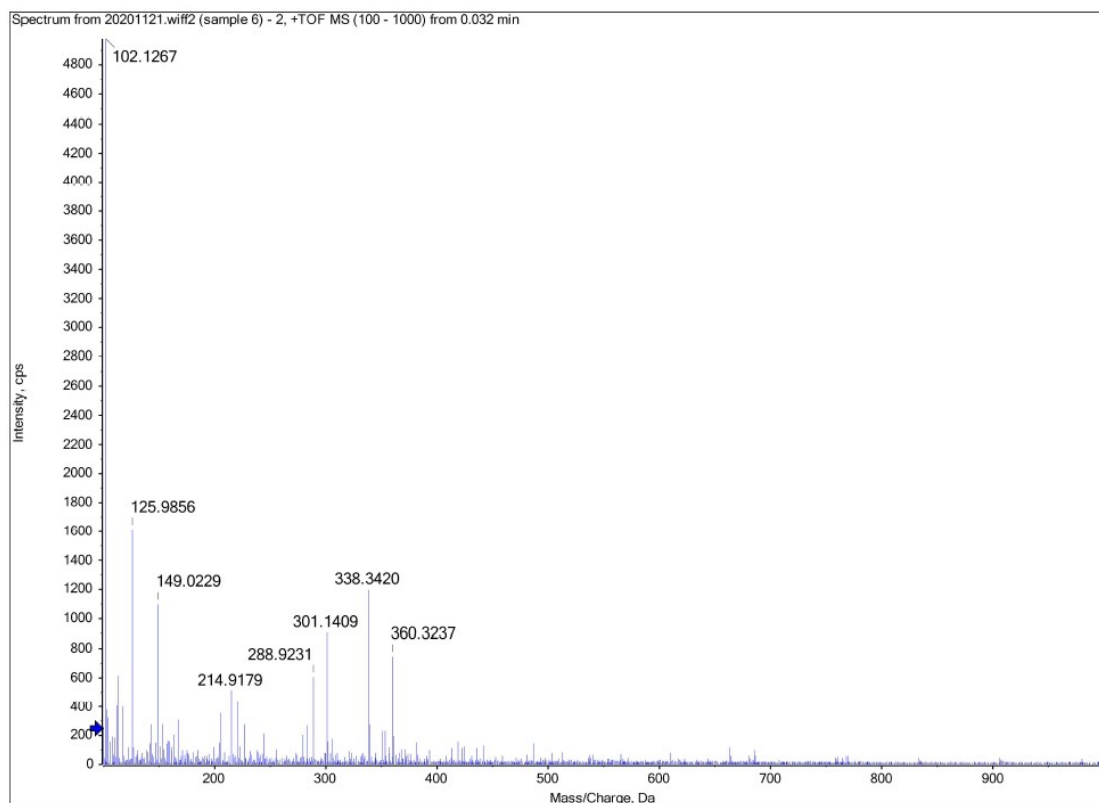


Figure S10. HR-MS (ESI) spectrum of **P5** after irradiation of 311 nm light.

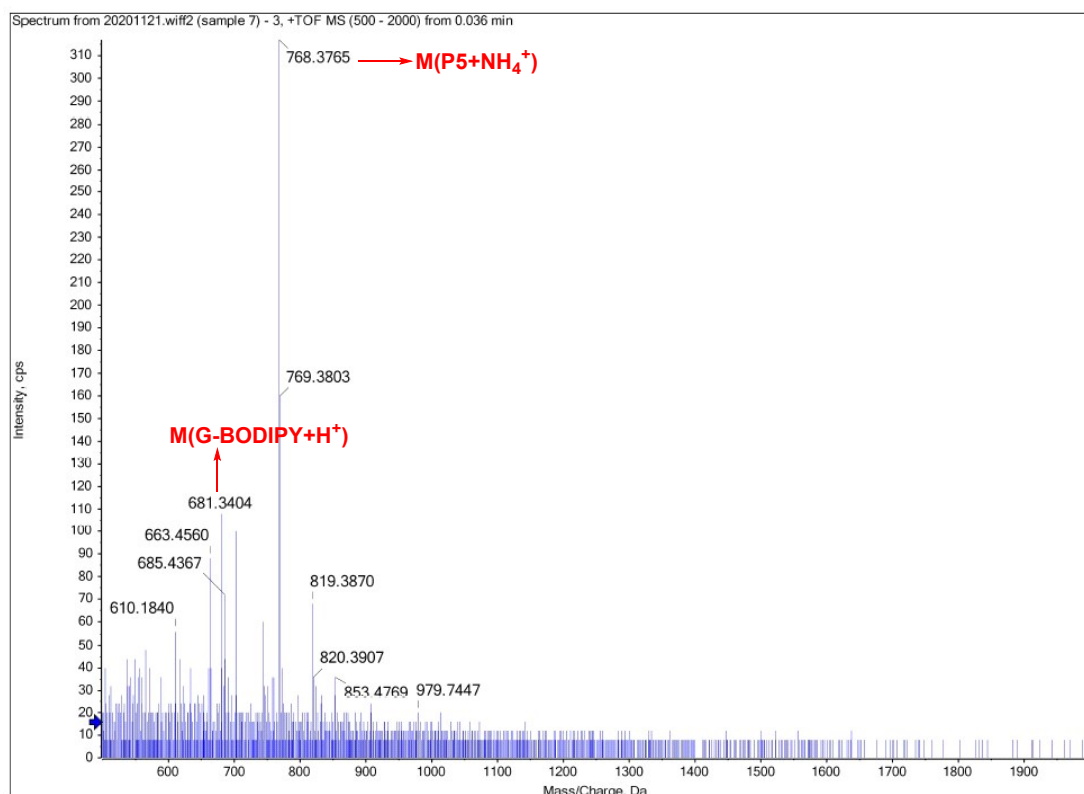


Figure S11. HR-MS (ESI) spectrum of **G-BODIPY-C-P5₂**.

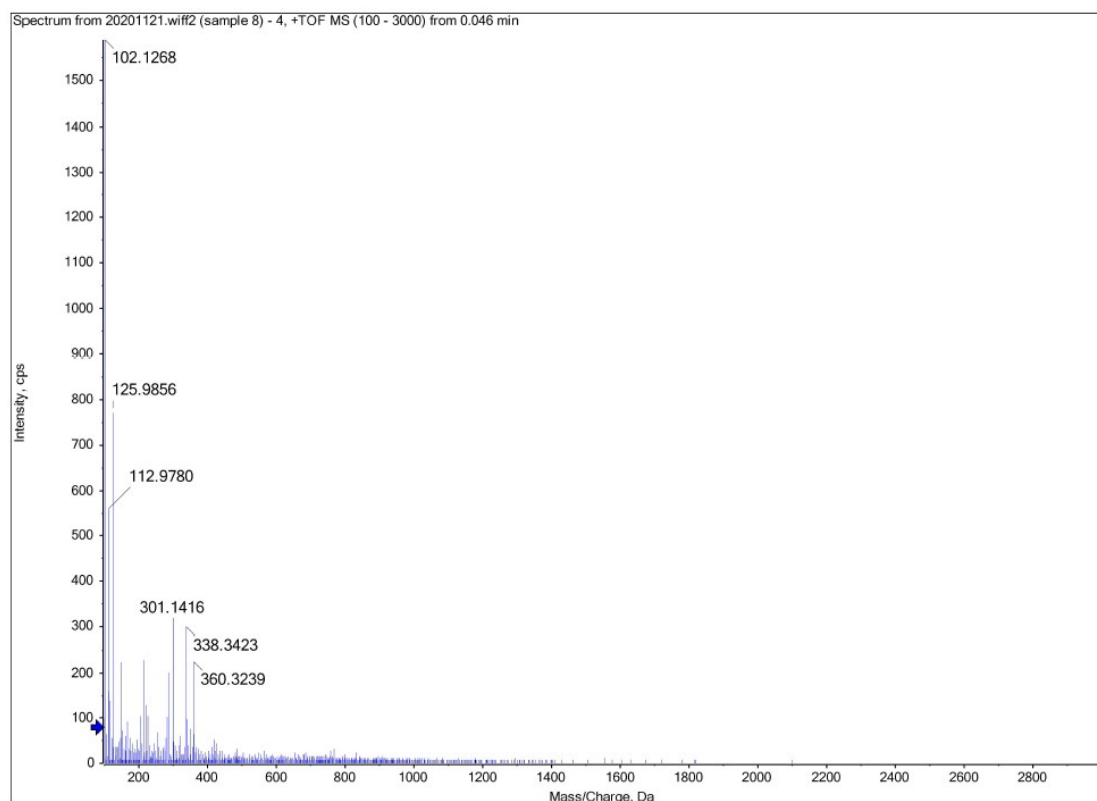


Figure S12. HR-MS (ESI) spectrum of **G-BODIPY-P5₂** after irradiation of 311 nm light.

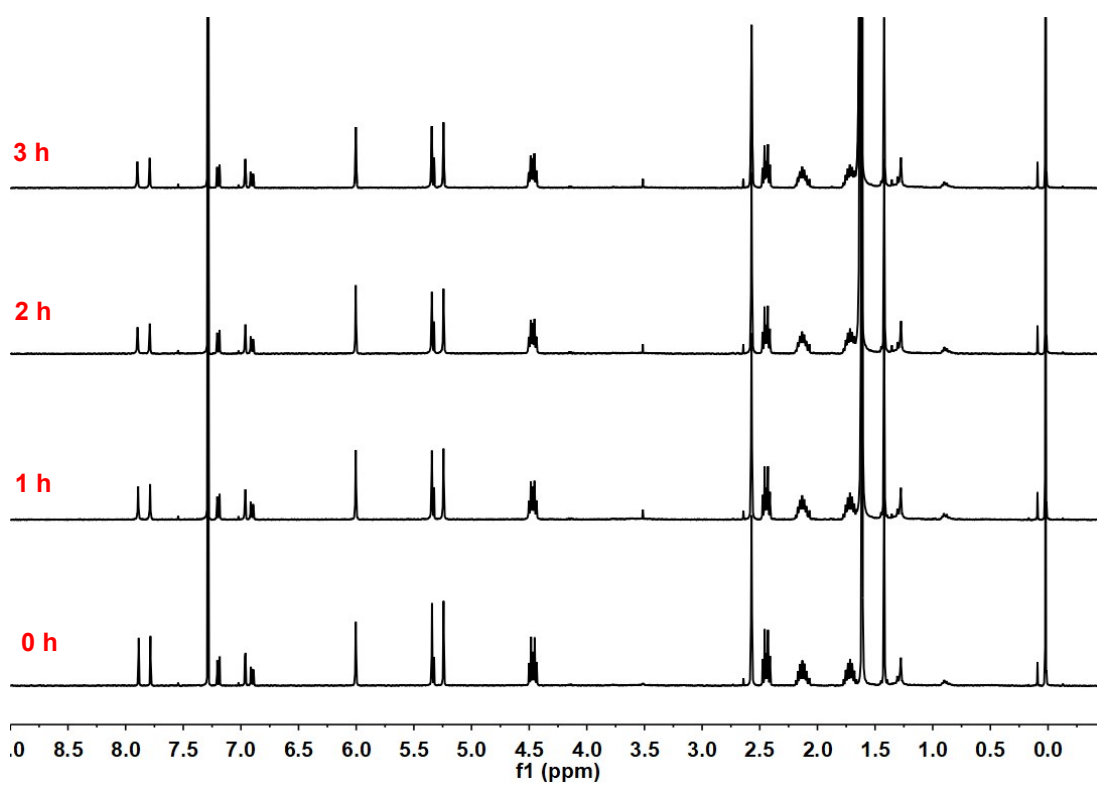


Figure S13. The variation of ¹H NMR (400 MHz, 298 K, CDCl₃) spectra of **G-**

BODIPY upon continuous irradiation of 311 nm for 1 h, 2 h and 3 h.

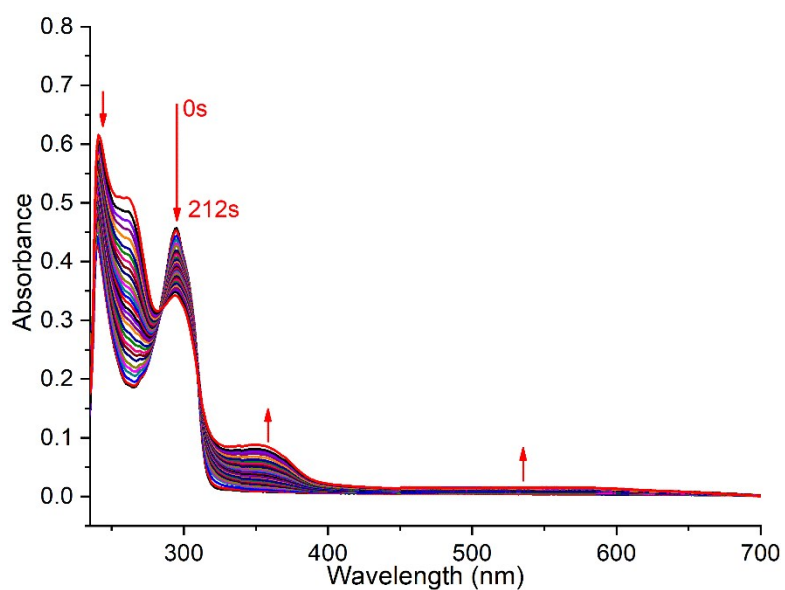


Figure S14. The variation of UV-vis absorption spectra of **P5** upon continuous irradiation of 311 nm light for 212 s; $[\mathbf{P5}] = 2 \times 10^{-5}$ mol/L.

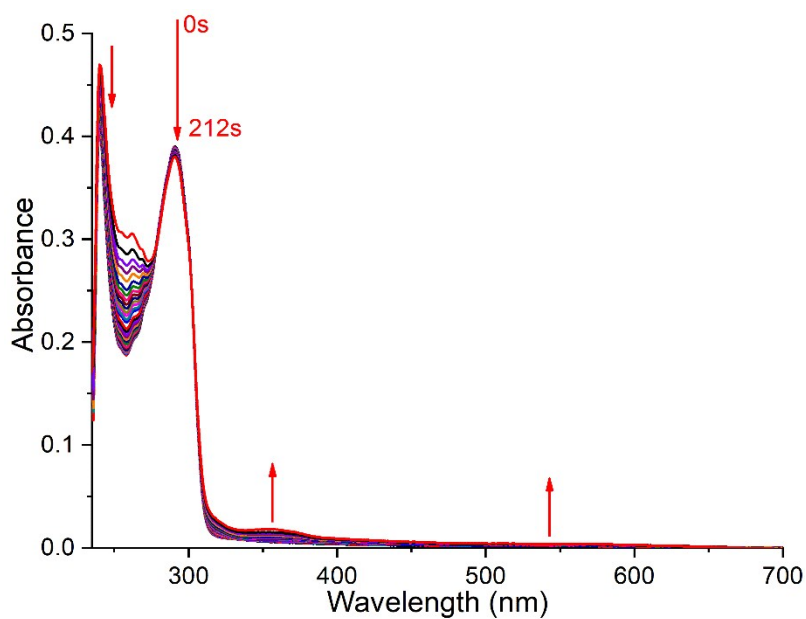


Figure S15. The variation of UV-vis absorption spectra of **PDME** upon continuous irradiation of 311 nm light for 212 s; $[\mathbf{PDME}] = 1 \times 10^{-4}$ mol/L.

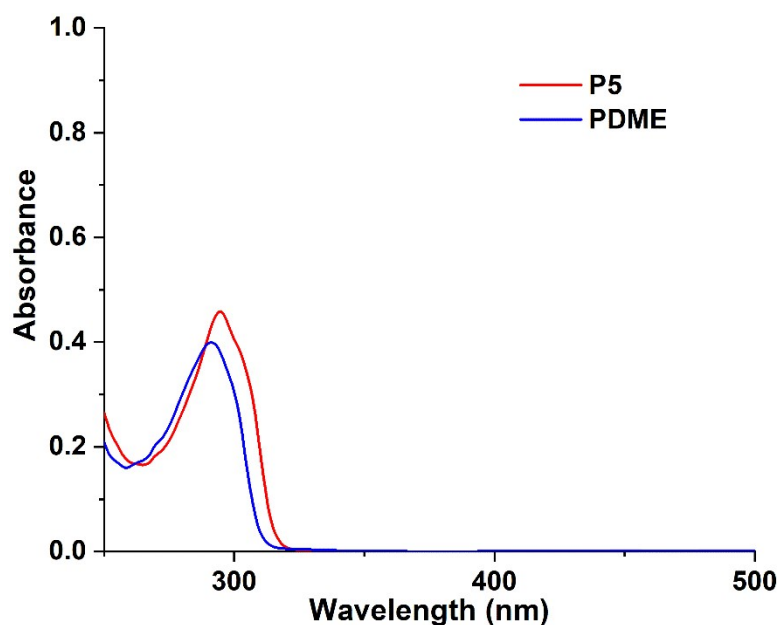


Figure S16. The absorption spectra of **P5** and **PDME**; $[\text{PDME}] = 5[\text{P5}] = 1 \times 10^{-4}$ mol/L.

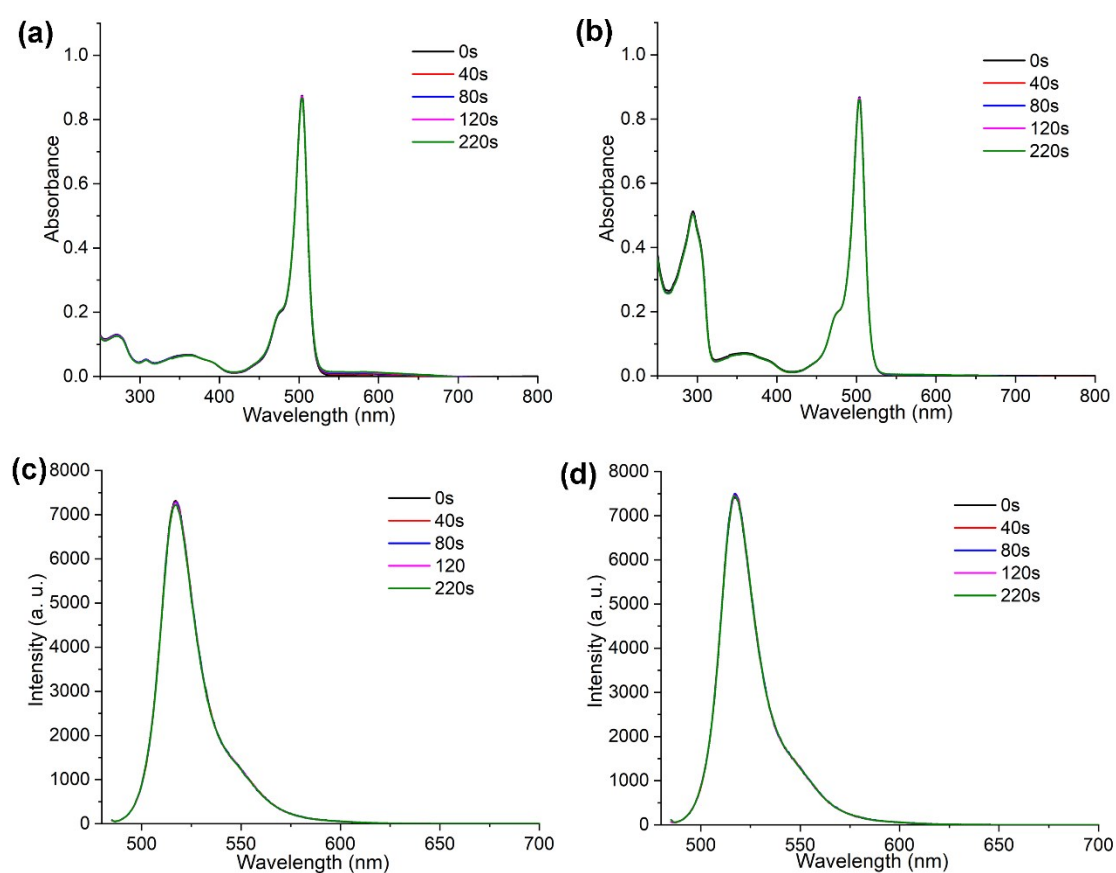


Figure S17. The variation of UV-vis absorption spectra of **G-BODIPY** (a) and **G-BODIPY-P5₂** (b) upon continuous irradiation of 500 nm light for 220 s; The variation

of fluorescence spectra of **G-BODIPY** (c) and **G-BODIPY**-**P5**₂ (d) upon continuous irradiation of 500 nm light for 220 s; $[P5] = 2[G-BODIPY] = 2 \times 10^{-5}$ mol/L; Excitation at 480 nm; Slit = 1, 2.5.

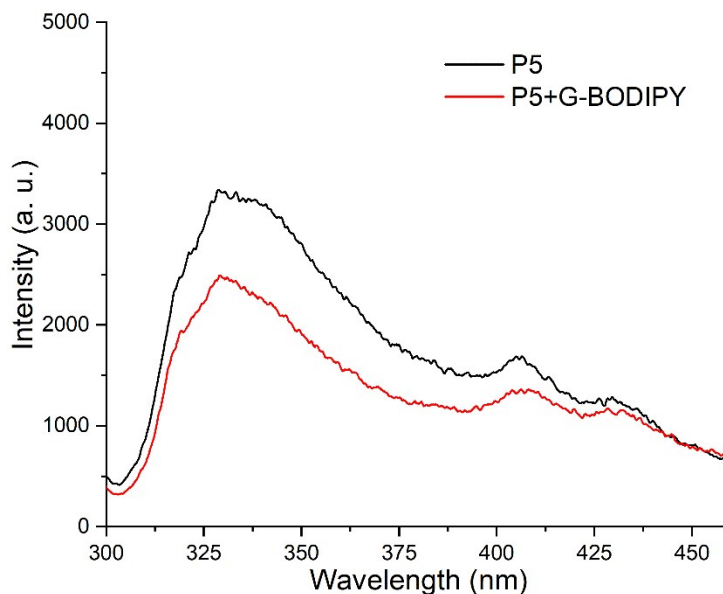


Figure S18. The fluorescence spectra of **P5** and **G-BODIPY**-**P5**₂; $[P5] = 2[G-BODIPY] = 2 \times 10^{-5}$ mol/L; Excitation at 285 nm; Slit = 5.0, 5.0.

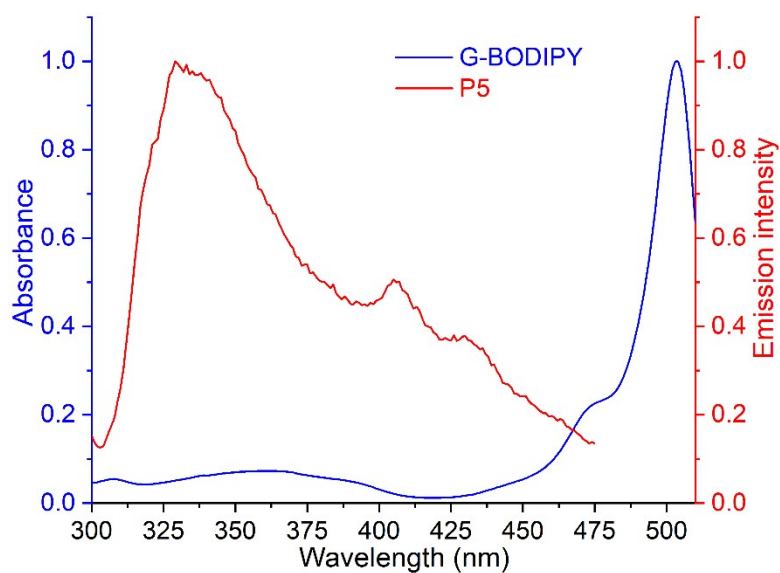


Figure S19. Spectral overlap of the absorption of **G-BODIPY** and the fluorescence emission of **P5**.

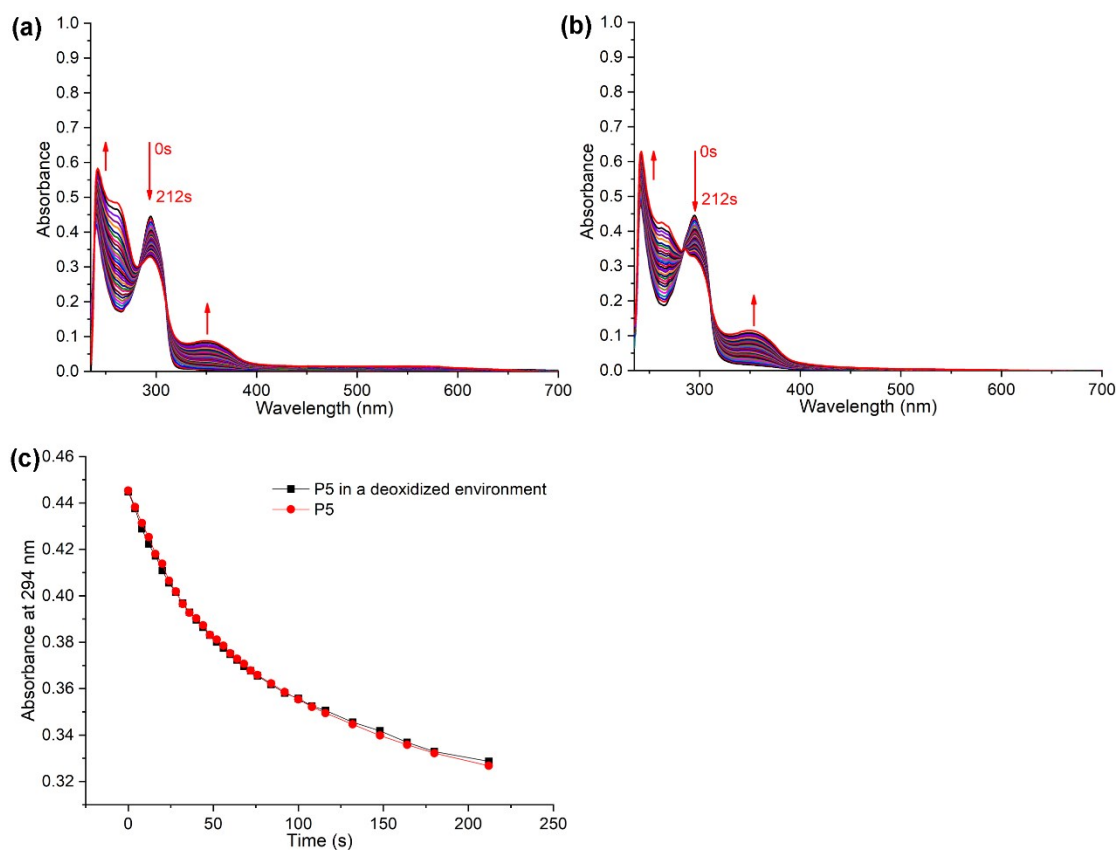


Figure S20. (a) The variation of UV-vis absorption spectra of **P5** in an oxygenated environment upon continuous irradiation of 311 nm light for 212 s. (b) The variation of UV-vis absorption spectra of **P5** in a deoxidized environment upon continuous irradiation of 311 nm light for 212 s. (c) The variation of absorbance of P5s in an oxygenated environment and a deoxidized environment at 294 nm with irradiation time of 311 nm light for 212 s. ($[P5] = 2 \times 10^{-5}$ mol/L)

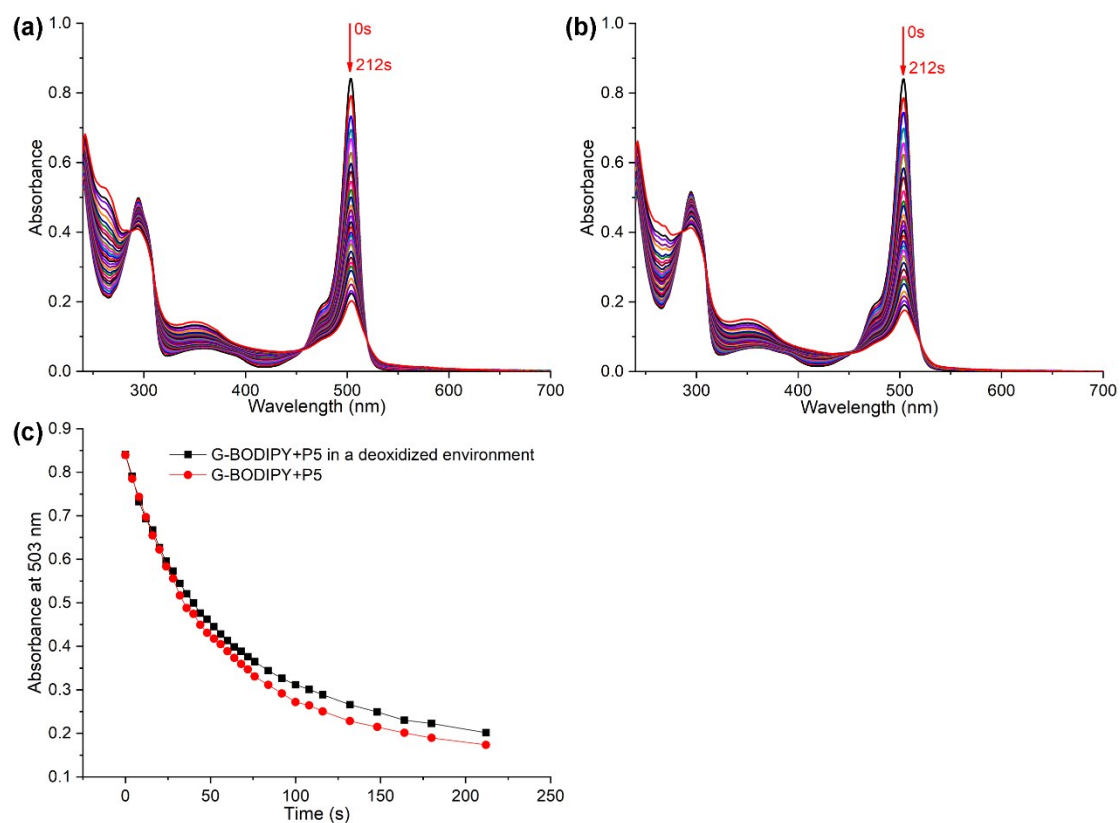


Figure S21. (a) The variation of UV-vis absorption spectra of **G-BODIPY-P5₂** in an oxygenated environment upon continuous irradiation of 311 nm light for 212 s. (b) The variation of UV-vis absorption spectra of **G-BODIPY-P5₂** in a deoxidized environment upon continuous irradiation of 311 nm light for 212 s. (c) The variation of absorbance of **G-BODIPY-P5₂** in an oxygenated environment and a deoxidized environment at 503 nm with irradiation time of 311 nm light for 212 s. ($[P5] = 2[G-BODIPY] = 2 \times 10^{-5} \text{ mol/L}$)

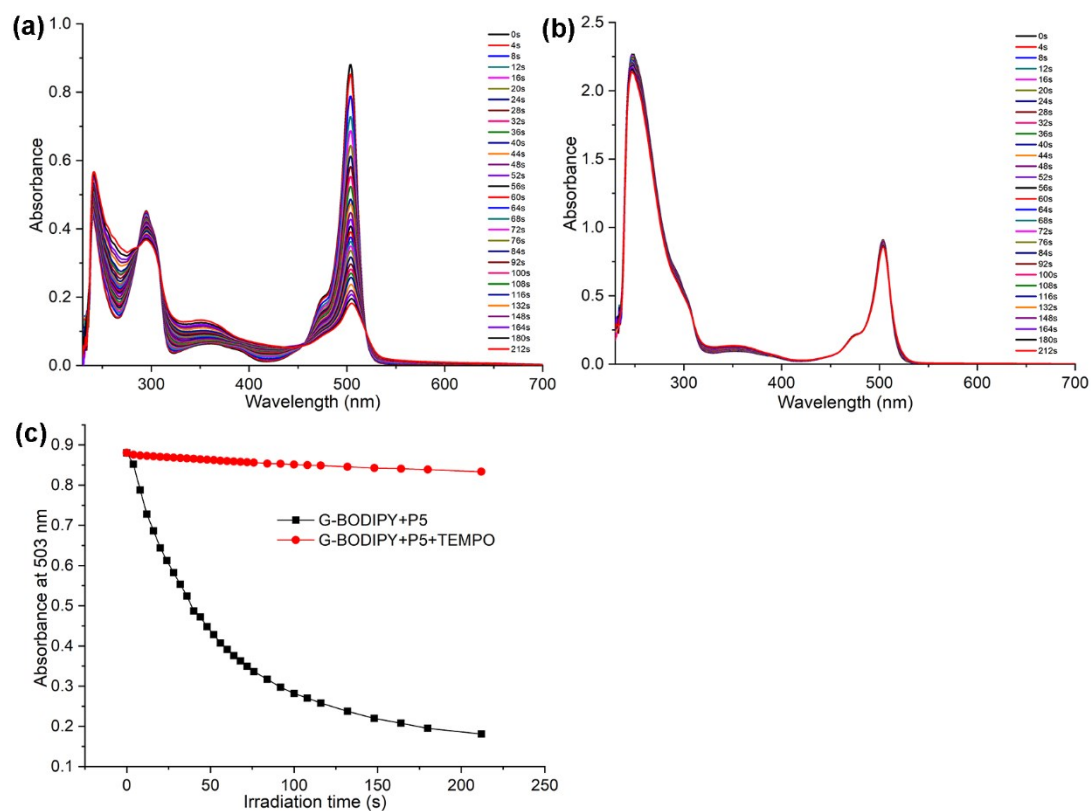


Figure S22. (a) The variation of UV-vis absorption spectra of **G-BODIPY**-**P5**₂ in absence of TEMPO upon continuous irradiation of 311 nm light for 212 s. (b) The variation of UV-vis absorption spectra of **G-BODIPY**-**P5**₂ in presence of TEMPO upon continuous irradiation of 311 nm light for 212 s. (c) The variation of absorbance of **G-BODIPY**-**P5**₂ at 503 nm in absence of TEMPO and in presence of TEMPO with irradiation time of 311 nm light for 212 s. ($[\text{P5}] = 2[\text{G-BODIPY}] = 2 \times 10^{-5} \text{ mol/L}$, $[\text{TEMPO}] = 1 \times 10^{-4} \text{ mol/L}$).

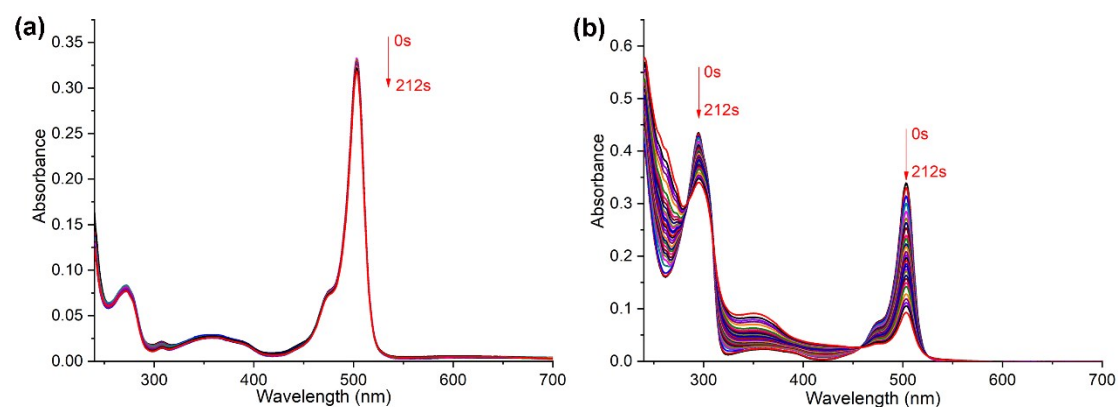


Figure S23. The variation of UV-vis absorption spectra of **4** (a) and **4+P5** (b) upon

continuous irradiation of 311 nm light for 212 s; $[P5] = 2[4] = 2 \times 10^{-5}$ mol/L.

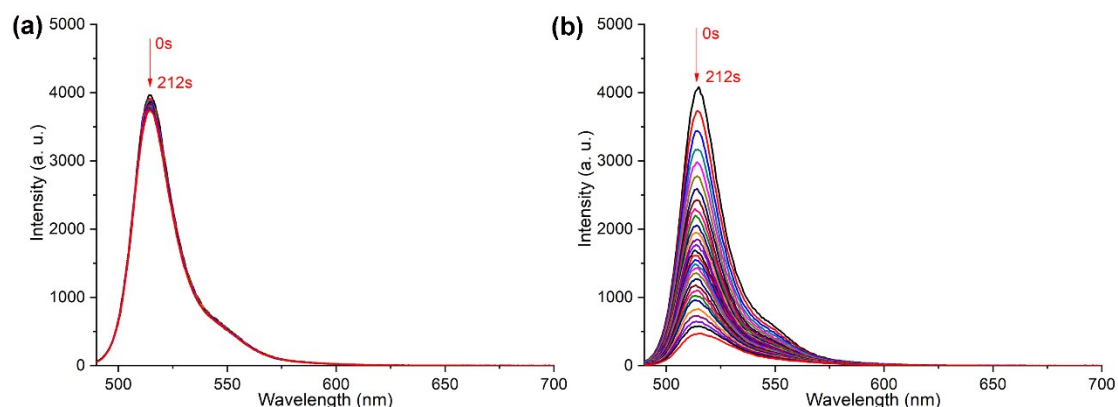


Figure S24. The variation of fluorescence emission spectra of **4** (a) and **4+P5** (b) upon continuous irradiation of 311 nm light for 212 s; $[P5] = 2[4] = 2 \times 10^{-5}$ mol/L.

*Association constant (K_a) determination for the complexation between **G** and **H**.²*

In addition to the corresponding signals for the uncomplexed **H** and **G**, a new species has occurred in the mixed solution of **G** and **H** in $CDCl_3$, indicating slow exchange on the NMR timescale. And the forces stabilizing the complex are very significant, since the percentage of the free guest is very small in the presence of **H** host. From integrations of all peaks, the stoichiometry of the complex was determined to be 2: 1. The association constant (K_a) can be determined using the 1H NMR single point method since the NMR response is slow on the NMR timescale. At low concentrations, such as 1.6 mM, the percentage of the free guest is larger than 50% in the presence of 1.0 eq. **H** host, which is inside the limits of the Weber rule that such determinations should be done within the limits of 20–80% complexation. The K_a values for **G** \subset **H** complex were determined to be $5.66 \times 10^6 M^{-2}$.

$$K = \frac{[G \cdot 2H]}{[G][H]^2}$$

References

1. T. Ogoshi, S. Kanai, S. Fujinami, T.-a. Yamagishi, and Y. Nakamoto, *J. Am. Chem.*

Soc., 2008, **130**, 5022 - 5023.

2. (a) L. Liu, N. Zhao and O. A. Scherman, *Chem. Commun.*, 2008, 1070-1072;
(b) W. Zhang, Y.-M. Zhang, S.-H. Li, Y.-L. Cui, J. Yu and Y. Liu, *Angew. Chem. Int. Ed.*, 2016, **55**, 11452-11456. (c) L. Ma, S. Wang, C. Li, D. Cao, T. Li and X. Ma, *Chem. Commun.*, 2018, **54**, 2405-2408.